

Chemical Synthesis And Characterization Of Lanthanum Oxide Nanoparticle Extended By Machine Learning Prediction

Pooja Shrivastava^{1*}, Vijay Kumar Baliyan², Bhavana Singh³

¹School of Sciences, Sanjeev Agrawal Global Educational University, Bhopal (M.P.)India

²School of Sciences, Sanjeev Agrawal Global Educational University, Bhopal (M.P.)India

³Department of Applied Physics, Jabalpur Engineering College, Jabalpur (M.P.) India

*Corresponding Author: Pooja Shrivastava

*poojadeveloped@gmail.com

Abstract: Low-cost co-precipitation method has used to synthesis the La_2O_3 nanoparticles at room temperature. The regression-based prediction model for estimating the optimal crystal size and respective strain has also presented. Energy Dispersive X-ray Spectroscopy (EDS), Scanning Electron Microscopy (SEM), Fourier Transform Infrared (FTIR) spectroscopy, and X-ray diffraction (XRD) were used to characterize the nanoparticles. With a particle size of 7.13nm and 7.92nm, a hexagonal structure has been formed, confirmed by XRD analysis. FTIR spectroscopy verified the existence of La-O stretching modes. The SEM images revealed the annealing effect on grain size and their agglomeration. The elemental composition of nanoparticles was determined by EDS analysis. The resulting nanoparticles morphology and properties were significantly influenced by the annealing temperature. Proposed method offers R^2 value of 0.9836 justifying the effectiveness of prediction.

Key Words: Nano particles, co-precipitation method, Machine Learning

1. INTRODUCTION

Particles with a size between 1 and 100 nm are called nanoparticles (NPs). Because of their exceptional physical and chemical characteristics, which set them apart from bulk materials, nanomaterials are becoming increasingly important in a wide range of applications [1]. Lanthanum oxide (La_2O_3) based nanoparticles are getting substantial attention in materials research due to their distinctive characteristics and prospective uses in numerous industries. N. Ramjeyanthi et al [1] in 2018. In the case of low-temperature usage, especially magnetic refrigeration, the magnetocaloric effect is an important factor to take into account. For materials like Tb_2O_3 and Dy_2O_3 nanoparticles, this effect, this depends on entropy changes brought on by magnetic fields. It is noticeable in cryogenic temperature ranges [2]. Because they use less energy and have a smaller environmental impact than traditional cooling systems, these effects are being thoroughly studied as alternatives. Undoped lanthanum oxide La_2O_3 nanoparticles offer advantages over Tb_2O_3 and Dy_2O_3 , including low toxicity to aquatic organisms and improved structural and optical properties. However, there isn't much specific studies reported on un-doped La_2O_3 nanoparticles. In recent times research is motivated towards utilizing the synthesis results to design machine learning (ML) based prediction to investigate the optimal crystal size and strain. Since broader peak in XRD can also indicate increased strain or defects within the crystal structure. This can affect the mechanical strength and stability of the nanoparticles. Thus, it is required to accurately predict the optimal synthesis parameters and is the one scope of this study.

The La_2O_3 nanoparticles have garnered significant attention in materials science due to their unique properties and potential applications. The preparation temperature profile has an impact on the synthesis of La_2O_3 nanoparticles as reported by S. Karthikeyan et al [3]. While moderate-temperature profiles produce well-defined NPs with enhanced crystallinity, low-temperature profiles lead to incomplete production. Larger, more crystallinity-producing NPs are encouraged by high-temperature profiles; yet, agglomeration and morphological loss may result at high temperatures. Extremely high temperature profiles have the potential to induce notable morphological and growth alterations. Because of its special qualities and prospective uses in a variety of industries, La_2O_3 nanoparticles have attracted a lot of interest in materials research. Therefore, this research paper aims to cover the synthesis for La_2O_3 nanoparticles using a simple and cost-effective co-precipitation method. By exploring different annealing temperature (160°C, 190°C), this work offers valuable insights into the impact of temperature on nanoparticle morphology, crystallinity, and properties.

2. CHALLENGE OF SYNTHESIS OF NANO PARTICLES

There are many challenges to be addressed for the successful synthesis of Lanthanum Oxide Nanoparticles. The multifaceted nature of synthesizing La_2O_3 nanoparticles is not merely a chemical reaction but a complex process requiring careful management of environmental factors, temperatures, and the inherent properties of the material to achieve the desired outcome. Most essential challenges are as follows and are illustrated in the Figure 1.

- **High Reaction with Moisture and CO_2 :** Lanthanum oxide is highly reactive with atmospheric moisture and carbon dioxide, requiring strict control of the synthesis environment.
- **Need for High Temperatures:** High temperatures are required for the synthesis of La_2O_3 nanoparticles, posing energy consumption and equipment limitations.
- **Reliability and Scalability Challenge:** Consistency in production and the ability to increase yield while maintaining quality are crucial for commercial applications.



Fig. 1 challenges in the synthesis of nanoparticles of lanthanum oxide

- **Security and Management:** Proper safety protocols and material management are essential when working with these compounds.
- **Nanoparticle Agglomeration Challenge:** Preventing or reducing agglomeration is crucial for achieving desired performance characteristics.
- **Control of Particle Dimensions and Morphological Challenge:** Providing precise control over the size, shape, and overall morphology of the nanoparticles is a critical challenge.

The creation of nanoparticles has historically been dominated by chemical and physical techniques. However, they frequently have drawbacks including the requirement for strong reaction conditions and environmental problems. Green synthesis techniques, which create nanoparticles using biological entities like bacteria and plants, are therefore gaining popularity. Although these green techniques are thought to be more sustainable and ecologically benign, they do have drawbacks, such as the need to scale up for big production and maintain stability through synthesis [7,8]. Therefore, this paper is aimed to successfully synthesize the nano particles by chemical route and annealed at different temperatures.

3. REVIEW OF SYNTHESIS OF NANO PARTICLES

Shinde et al. [2] investigated the magnetocaloric effects in La_2O_3 materials. While P Ram Kumar et al. [4] looked into the hydroxyl radical scavenger action of La_2O_3 nanoparticles, highlighting their biological significance; S. Karthikeyan et al. [3] explored the effects of elevated temperatures on La_2O_3 nanostructures. S. Rahul obtained an interesting result suggesting the apparent increase in crystalline nature as the synthesis time was extended confirmed by XRD [5]. Ismail et al [6] have synthesized lanthanum oxide La_2O_3 nanoparticles NPs by laser ablation in water without using surfactant, they were tried to find the effect of laser wavelength on the optical and structural properties of La_2O_3 NPs. The study of mycogenic nanoparticles, their fungal manufacture, and

their uses in environmental cleanup and medicine, Khandel and Shahi [7] highlight the difficulties and current state of using these biogenic materials.

Numerous green synthesis techniques, such those used by Joshi et al. [9], with leaf extract from *Syzygium cumini* and with *Cannabis sativa* [8], show the tendency toward ecologically benign ways to produce nanoparticles. New methods for La_2O_3 nanoparticles targeted for CMOS applications that use propylene glycol and glutaric acid Pathan et al. [10]. By rigorously analysing the Scherrer and Debye-Scherrer equations, Holzwarth and Gibson [11] advanced our knowledge of how to determine the size of nanoparticles using X-ray diffraction techniques. The basic work in crystallite size analysis by Williamson and Hall [12] is still relevant in today's research. Anu Krishna and Tharayil [13] highlighted the suitability of La_2O_3 nanoparticles for electrical applications by concentrating on their dielectric characteristics after synthesizing them using chemical co-precipitation. Examining the synthesis and optical characteristics of different lanthanum hydroxide as well as oxide NP's, Mu and Wang's work [14] focused on shape-preserved changes, which are essential for customizing material properties. Furthermore, La_2O_3 nanoparticles' capacity to scavenge hydroxyl radicals was examined by P Ram Kumar et al. [15], suggesting that they may find use in biomedical applications. Collectively, these investigations highlight the adaptability and importance of lanthanum oxide nanoparticles in a variety of scientific domains.

Jayadeep Tejani et al. [16] presented a controlled synthesis of lanthanum nanorods [16] serves as another example of how nanoparticle morphology may now be tailored for certain uses. Glutaric acid as well as propylene glycol were used in a synthesis method created by Pathan et al. [17] to improve the material's characteristics for CMOS applications. Furthermore, new synthesis pathways utilizing glutaric acid and combustion techniques, respectively, were introduced by investigations such as those of Khalaf & Al-Mashhadani [18]. Applications in cutting-edge technology and production techniques have been the main topics of recent studies on lanthanum oxide La_2O_3 nanoparticles. Metal-oxide nanomaterials, such as those based on lanthanum, were investigated by Yeosang Yoon et al. [19] in flexible sensors for environmental and health monitoring. In their study of the controlled production of lanthanum nanoparticles, Tejani et al. [20] shed light on their structural characteristics and potential uses in catalysis and electronics.

Current reviews, such as Bhautik's [21], highlight the continuous research in this field by summarizing several synthesis and characterisation methods for La_2O_3 . The biological uses and photocatalytic capabilities of La_2O_3 nanoparticles are further investigated in studies by Hanif et al. [22] as well as Pranali S. Parab et al. [23]. Novel manufacturing techniques and catalytic uses have been brought to light by recent research on lanthanum oxide nanoparticles. A unique method for creating La_2O_3 nanoparticles using nano-sized lanthanum (III) molecules was presented by Parimala Gandhi et al. [24]. Tao et al. [25] examined methods for data-driven synthesis optimization and investigated the incorporation of ML methods in nanoparticle synthesis. In order to show the potential of La_2O_3 in catalytic applications and environmental remediation, Velinova et al. [26] studied the synthesis and characterisation of Pd/ La_2O_3 / ZnO catalysts for the oxidation for methane, propane, along with butane. Together, these pieces demonstrate the various techniques and uses of La_2O_3 nanoparticles, opening the door to novel applications in environmental remediation, catalysis, and nanomedicine. The Table 1 have presented the summary of the various Nanoparticle synthesis literature summary.

Table. 1 Survey for Nanoparticle synthesis and methods

| Reference | Methodology | Nanoparticle | Synthesis Method |
|--------------------------|-----------------------------|---|--|
| N. Ramjeyanthi et al [1] | Co-precipitation | La_2O_3 | Co-precipitation method |
| Shinde et al [2] | Magnetocaloric effect | Tb_2O_3 , Dy_2O_3 | Rare earth nitride formation and successive oxidation |
| S. Karthikeyan et al [3] | Temperature effects | La_2O_3 nanostructures | Simple Reflux Method |
| P Ram Kumar et al [4] | Hydroxyl radical scavenging | La_2O_3 | Co-precipitation and Field emission scanning electron microscopy (FESEM) |
| Khandel & Shahi [7] | Mycogenic applications | Mycogenic nanoparticles | Mycogenesis of nanoparticles |
| Ahmadi & Lackner [8] | Green synthesis | Silver | Green synthesis from <i>Cannabis sativa</i> |
| Joshi et al [9] | Green synthesis | $\alpha\text{-Fe}_2\text{O}_3$ | Leaf extract of <i>Syzygiumcumini</i> |

| | | | |
|-------------------------------|----------------------------------|---|--|
| Pathan et al [10] | Glutaric acid & propylene glycol | La ₂ O ₃ | Chemical synthesis |
| P. G. Anu Krishna et al [13] | Dielectric properties | La ₂ O ₃ | Co-precipitation method |
| Qiuying Mu & Yude Wang [14] | Shape-preserved transformation | La(OH) ₃ , La ₂ O ₂ CO ₃ , La ₂ O ₃ | A chemical synthesis (or facile process) |
| Jayadeep Tejani et al [16] | Controlled synthesis | Lanthanum NR's | Controlled synthesis |
| Khalaf & Al-Mashhadani [18] | New combustion method | La ₂ O ₃ net-like | Combustion method |
| Hanif et al [22] | Citrus aurantium extract | La ₂ O ₃ | Chemical synthesis |
| Pranali S. Parab et al [23] | Doping and coating | La ₂ O ₃ | Green synthesis approach |
| K. Parimala Gandhi et al [24] | Novel synthesis | La ₂ O ₃ | Sono-chemical method and (FESEM) |
| Tao et al [25] | Machine learning-assisted | Various nanoparticles | Co-precipitation and Machine learning techniques |
| Velinova et al [26] | Catalyst development | Pd/La ₂ O ₃ /ZnO | catalytic oxidation with palladium deposition |

Table 1 summarizes various methodologies employed in the synthesis of nanoparticles, highlighting a range of materials and techniques used by different researchers with co precipitation method highly referred.

4. SYNTHESIS PROCESS AND STEPS

The sequential steps involved in the synthesis of La₂O₃ nanoparticles using the chemical Co precipitation method, are as described below,

- The powder of Lanthanum Nitrate Hexa Hydrate (La(NO₃)₃ · 6H₂O) & Sodium Hydroxide (NaOH) are the basic precursors used for the synthesis of the sample. Initially solution of 0.1M for lanthanum nitrate and of 0.3M for NaOH was prepared by mixing each in 100mL of distilled water in two separate beakers.
- The prepared solution of NaOH was drop wise added to the precursor solution of lanthanum nitrate kept on magnetic stirrer.
- The solution was agitated at normal temperature for 140 minutes with constant speed. At the beginning of the reaction the pH was found to be 12 and finally reaches up to 14 at the last.
- Now the solution was kept at rest for 8h, by which the precipitate was settled down at the bottom.
- Now remove the excess water from beaker and further cleaned multiple times with distilled water and once with ethanol.
- This cleaning process is followed by filtration and congregated in watch glass and then air dried till 96 hours at normal room temperature.
- Again, the sample was kept in electric oven at the temperature of 160 °C and 190°C for one hour separately. Lastly, the dried precipitate was crush into fine particles using mortar and pestle.

5. RESULTS

The XRD measurements are used to understand the qualitative analysis of sample. The X-ray diffraction pattern of Lanthanum oxide synthesised by co-precipitation method and annealed at 160°C and 190°C are shown in figure 2. One can conclude from the appearance of more than one prominent peak that the prepared lanthanum oxide samples are polycrystalline in nature. The main peaks observed at 2θ (deg.) 15.74°, 26.3°, 28.08°, 31.67° and 39.4° are in good agreement with JCPDS card no. 83-2034 (COD:4031381) corresponds to the hexagonal phase of La(OH)₃. Along with this extra peak around 30.1°, 40.0° and 48.7° is also observed, corresponds to pure La₂O₃ (JCPDS-05-0602) with hexagonal phase. At lower annealing temperature some traces of La(OH)NO₃ (COD:4344281) is also observed. The structural characterization of the synthesized nanoparticles was performed using X-ray diffraction (XRD) analysis [11, 12]. The fundamental XRD characterization is defined as;

$$n\lambda = 2d\sin(\theta) \quad (1)$$

Where, n stands for reflection order, λ is X-ray wavelength ($\lambda=1.5418\text{\AA}$), d is defined as interplanar spacing, and finally the θ is diffraction angle(or Bragg angle)at peaks. By utilizing the Debye-Scherrer equation (2) [11], the mean crystallite size (D in nm) for the La_2O_3 nanoparticles was determined as,

$$D = \frac{K \cdot \lambda}{\beta \cos(\theta)} \quad (2)$$

where K is set to as constant value of (0.94), and β is defined as full width of the half maxima(FWHM) Holzwarth et al. [11] and Williamson-Hall [12]. The mechanical strain is mathematically defined as;

$$\varepsilon = \beta / 4 \tan \theta \quad (3)$$

The values so obtained for grain size, inter-planner spacing, FWHM, Mechanical strain are presented in table2 given below. It is observed that on increasing the annealing temperature the particle size and mechanical strain increases.

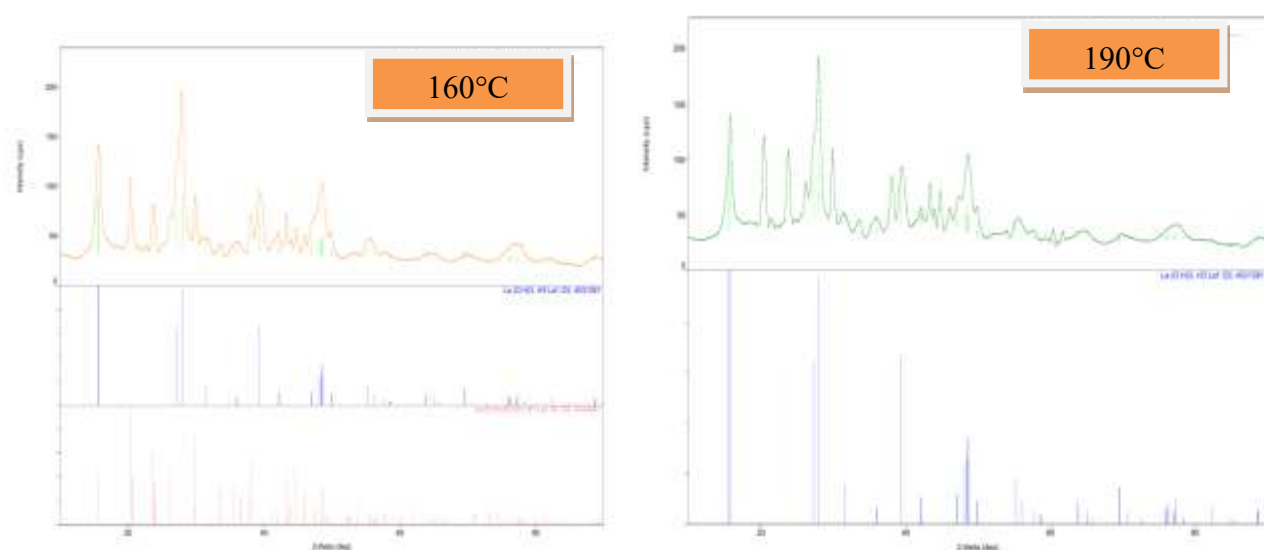


Figure2 XRD characterization results for samples annealed at 160 °C and 190°C.

| Compound | Temp. | JCPDS- 83-2034 (COD-4031381) | Obtained values for lattice para | Interplaner spacing d (\AA) | FWHM | Grain size (nm) | Mechanical Strain ε |
|--------------------------|-------|------------------------------|----------------------------------|--|------|-----------------|---------------------------------|
| $\text{La}(\text{OH})_3$ | 160°C | $a=b=6.547$ $c=3.85$ | $a=b=6.466$, $c=3.84$ | 3.17 | 1.20 | 7.13 | 0.02924 |
| $\text{La}(\text{OH})_3$ | 190°C | $a=b=6.547$ $c=3.85$ | $a=b=6.235$, $c=3.97$ | 3.23 | 1.08 | 7.92 | 0.051133 |

Table 2: Key parameters obtained by XRD analysis

When describing the creation of nanoparticles Fourier Transform Infrared (FTIR) spectroscopy is a useful tool to identify the presence of chemical bonding and functional group in the material. Certain vibrational modes experienced by the molecules in the sample are represented by the peaks and troughs within the spectrum at different wave numbers; the spectrum displays a number of notable peaks

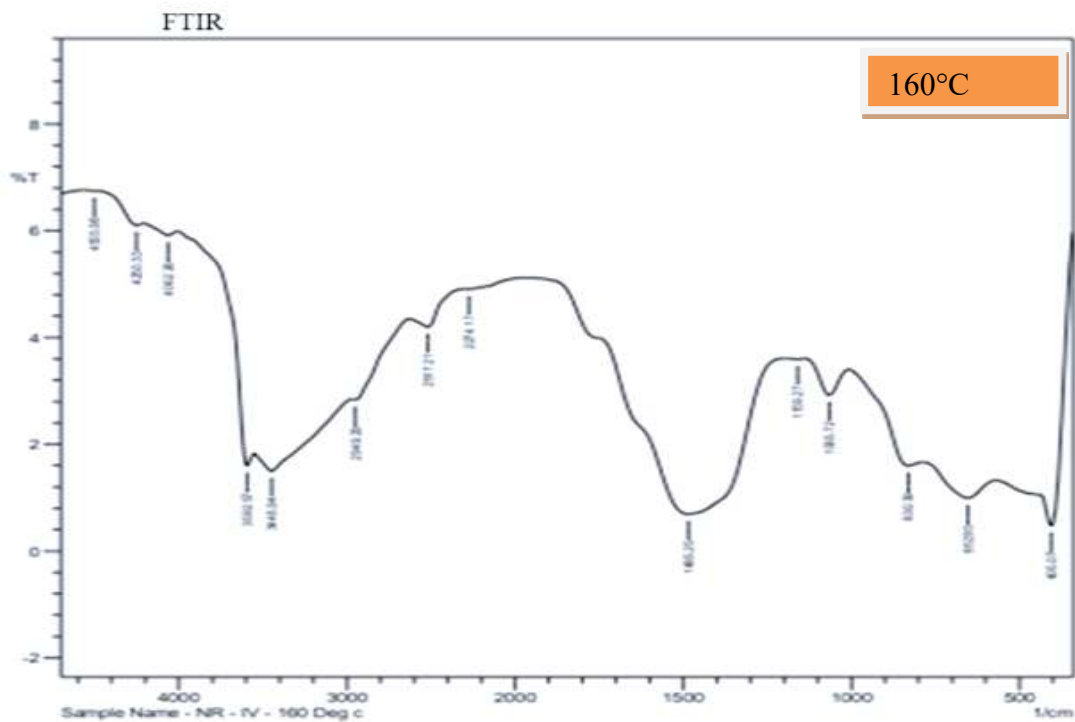


Figure 3 Results of the FTIR spectral peak analysis validated at 160 °C

The distinctive absorption bands for La-O stretching vibrations and peaks for hydroxyl groups as well as carbonate species that can appear during synthesis are usually visible in FTIR spectra of lanthanum oxide nanoparticles.

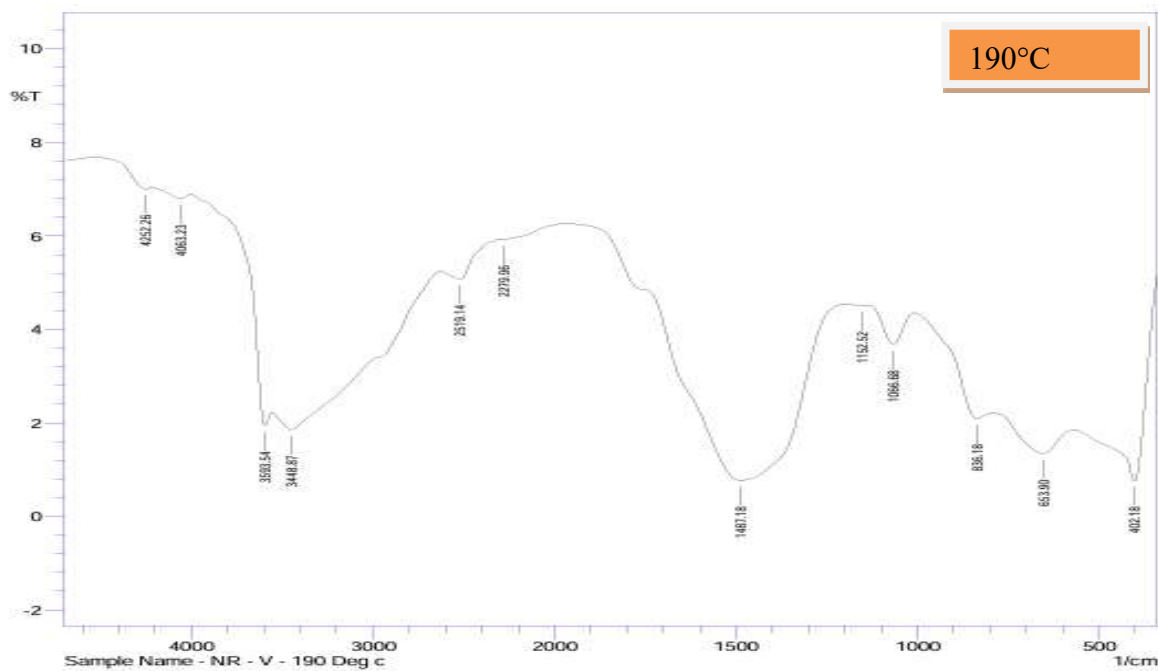


Figure 4 Results of the FTIR spectral peak analysis validated at 190 °C

| Wave number (cm ⁻¹) | Functional Group/Band Assignment | References |
|---------------------------------|----------------------------------|------------|
| 160°C190°C | | |

| | | | |
|---------|---------|--|---------|
| 2517.21 | 2519.14 | Single bond, hydrogen bond due to presence of H ₂ O | [1] |
| 2949.29 | 3448.87 | | |
| 3446.94 | 3593.54 | | |
| 3592.57 | 4063.23 | | |
| 4062.26 | 4252.26 | | |
| 2274.17 | 2279.96 | Triple bond, C_N | [2] |
| 1485.25 | 1487.18 | C-C stretching, or CH ₃ antisymmetric stretching | [2],[4] |
| 1065.72 | 1066.68 | C-OH, C-O stretching | [2],[4] |
| 1159.27 | 1152.52 | | |
| 830.39 | 836.18 | C-O banding | [3],[4] |
| 652.93 | 653.9 | La-O Stretching and bending | [1],[3] |
| 405.07 | 402.18 | | |

Table 3 Description of Wave Number vs Functional Groups material at 160°C and 190°C

The FTIR spectra in the wavenumber range 4000-400 cm⁻¹ of the as-prepared samples are shown in Fig.3,4. At the spectrums of the annealed samples at 160°C in Fig. 3, a broad band is observed at the wavenumber of 4062.26, 3592.57, 3446.94, 2949.29, 2517.21 cm⁻¹ respectively and these bands show the presence of O-H stretching vibration which may due to the presence of absorbed moisture on the surface of the samples [1]. The peak around 2274cm⁻¹ may due C-N triple bond [2]. The absorption peaks at around 1485, 1487 cm⁻¹ in the samples is found because of the asymmetric and symmetric stretching of CH₃and C-C bond respectively [2,4]. The band observed at 1159, 1152, 1065 and 1066 are due to C-OH, C-Ostretching vibration but in the same samples, the sharp absorption bands at around 830, 836 cm⁻¹ is owing to C-O bending vibration. The broad absorption bands at 652,653 cm⁻¹(F) in samples is observed because of the La-O stretching vibration while the small bands at 405 and 402 cm⁻¹ in the same samples is due to La-O bending vibration. The presence of above mentioned bands therefore confirmed the existence of La₂O₃ [1,3]. The location of all the band frequencies and their corresponding modes of vibration are recorded in Table 3 for better comparison.

Figure 5 presents scanning electron microscopy (SEM) images comparing the morphology of Lanthanum hydroxide synthesized at 160°C and at 190°C. Both SEM results show agglomerated nanoparticles. The sample annealed at 160°C appears to have slightly larger and less densely packed agglomerates compared to the 190°C sample, which exhibits smaller, more closely aggregated nanoparticles. The scale bar indicates a 1 µm scale for both images, allowing for a direct visual comparison of particle size and distribution.

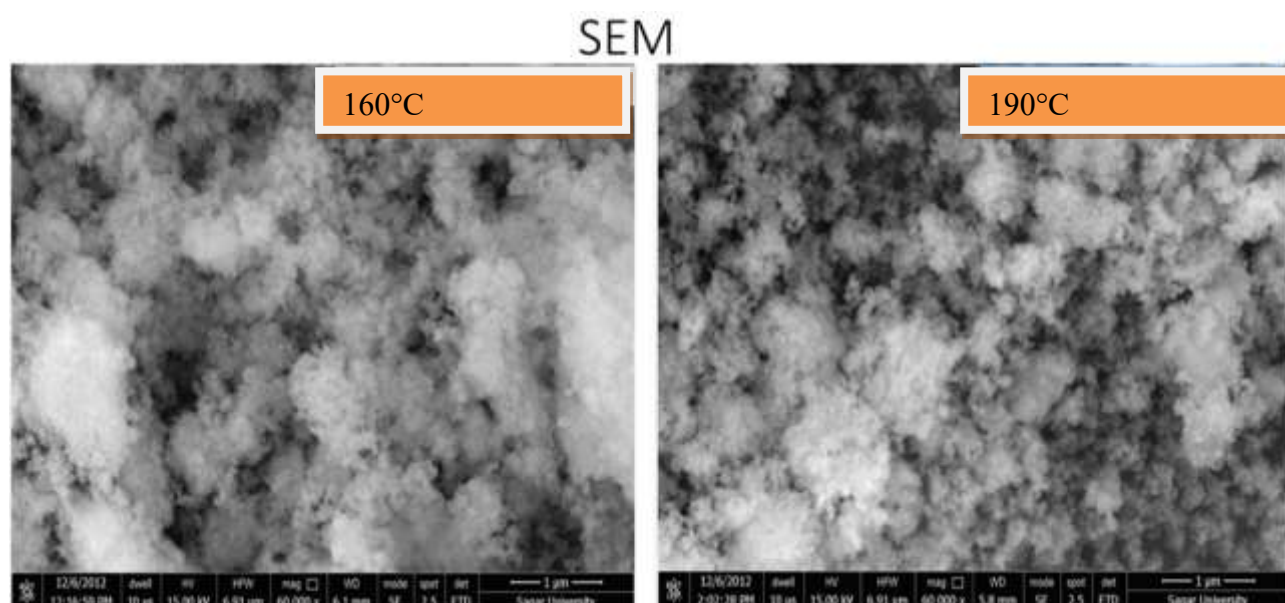


Figure 5 Results of the SEM analysis comparison

In order to Justify the statement, Figure 6a) and Figure 6b) present ultraviolet UV-Visible spectroscopy results for 160°C and at 190°C, respectively. Figure 6a shows a significant absorbance peak around 300 nm, followed by a gradual decrease in absorbance across the visible spectrum. Successful synthesis at 160°C is indicated by the La_2O_3 nanoparticle-specific peak at 300 nm in Figure 6a). On the other hand, Figure 6b) for $\text{La}(\text{OH})_3$ at 190°C shows a less pronounced absorption curve. This discrepancy in spectrum patterns points to differences in the two samples particle size, shape, or makeup, which might be examined further using complementary analytical methods like transmission electron microscopy etc.

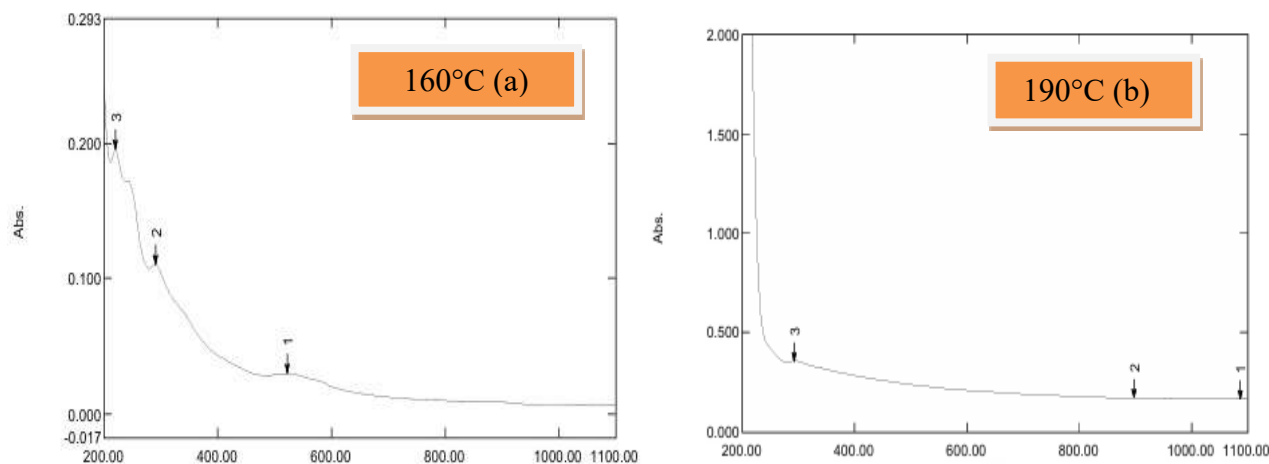


Figure 6(a,b) results of the UV-VISIBLE SPECTROSCOPY

Energy Dispersive X-ray Spectroscopy is an analytical technique used to characterize the elemental composition of materials, including nanoparticles. This section has presented the comparative analysis of the EDS analysis performed over the 160°C and 190°C temperatures for the proposed nanoparticles in conjunction to above shown SEM molecules. The Table 4 presents a comparison of atomic and weight concentrations of Lanthanum (La) and Oxygen (O) obtained from EDS analysis at two different low temperatures: 160°C and 190°C respectively. The data shows consistent results across both temperatures. The values so obtained are given in table 4. It is observed from the obtained data that with weight concentration of La increases while oxygen decreases.

| Element Number | Element Name | Element Symbol | at 160 degree C | | | at 190 degree C | | |
|----------------|--------------|----------------|-----------------|-----------------|----------------|-----------------|-----------------|----------------|
| | | | Atomic Concn. % | Weight Concn. % | Error in (wt%) | Atomic Concn. % | Weight Concn. % | Error in (wt%) |
| 57 | Lanthanum | La | 23.76 | 73.01 | 1.66 | 25.89 | 75.20 | 1.79 |
| 8 | Oxygen | O | 76.24 | 26.99 | 2.99 | 74.11 | 24.81 | 2.88 |

Table 4 comparison of %Atomic concentration forEDS analysis at low temperatures

EDS can be used to create elemental maps of the sample, showing the distribution of different elements across the surface of the nanoparticles. This information can be vital for understanding how the properties of nanoparticles might vary spatially. The qualitative results are presented in the Figure 7(a,b) for the two cases of EDS at 160 °C and 190 °C respectively.

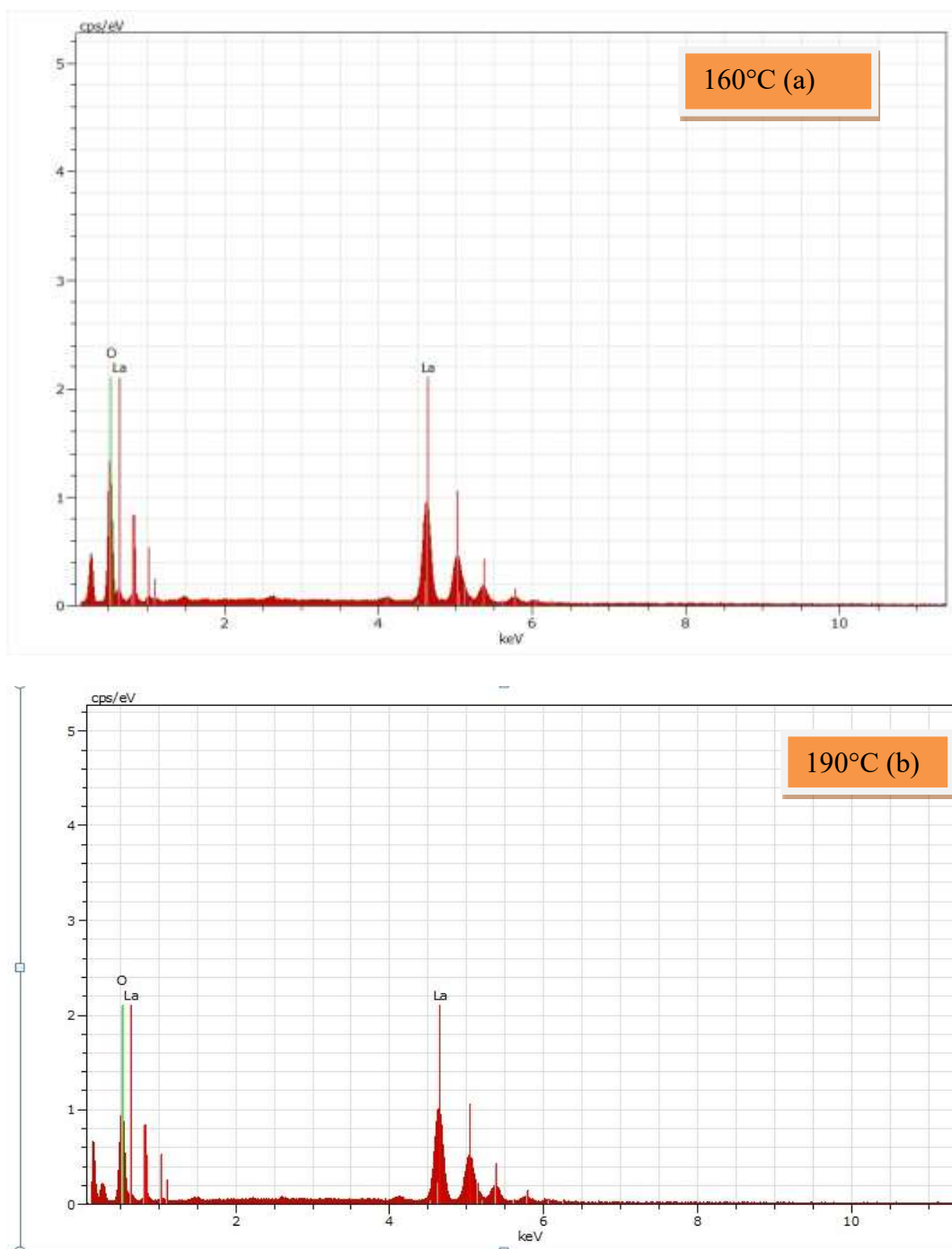


Figure 7(a,b) results of EDS spectrum of prepared samples

MACHINE LEARNING BASED PREDICTIONS AND ANALYSIS

This section presented the additional ML based MATLAB simulation to include X-ray Diffraction (XRD) characterization using the Debye-Scherrer formula, mechanical strain calculation, and crystalline parameters. This investigation includes specific parameters such as the shape factor K , X-ray wavelength λ , FWHM β , and the Bragg angle θ . The impact of the lower β factor is investigated and the respective ML based optimal strain and crystalline size is predicted. Table 5 presented the raw data used for the prediction of optimal β , strain ϵ , and Crystallite Size.

| Beta Value | Crystallite Size @ 160°C (nm) | Mechanical Strain @ 160°C | Crystallite Size @ 190°C (nm) | Mechanical Strain @ 190°C |
|------------|-------------------------------|---------------------------|-------------------------------|---------------------------|
| 0.05 | 2.87 | 0.0467 | 2.87 | 0.0467 |
| 0.07 | 2.15 | 0.0622 | 2.15 | 0.0622 |
| 0.08 | 1.72 | 0.0778 | 1.72 | 0.0778 |
| 0.10 | 1.43 | 0.0933 | 1.43 | 0.0933 |
| 0.12 | 1.23 | 0.1089 | 1.23 | 0.1089 |
| 0.13 | 1.08 | 0.1244 | 1.08 | 0.1244 |
| 0.15 | 0.96 | 0.1400 | 0.96 | 0.1400 |
| 0.17 | 0.86 | 0.1555 | 0.86 | 0.1555 |
| 0.18 | 0.78 | 0.1711 | 0.78 | 0.1711 |
| 0.20 | 0.72 | 0.1866 | 0.72 | 0.1866 |

Table 5 Results of the ML based prediction of crystalline size and Strain

The linear regression model is applied over the data to predict the optimal size and strain. the mathematical made; is illustrated by

$$y = -0.0631x + 0.2038 \quad (4)$$

The third order prediction for polynomial regression is mathematically modelled as;

$$y = p_1x^2 + p_2x + p_3 \quad (5)$$

$$y = 0.0385x^2 + -0.1970x + 0.2986 \quad (6)$$

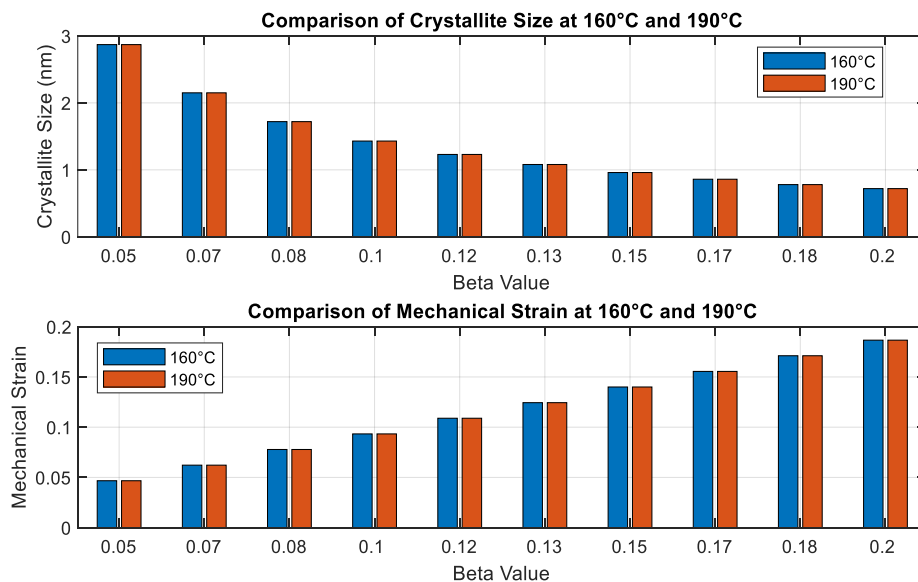
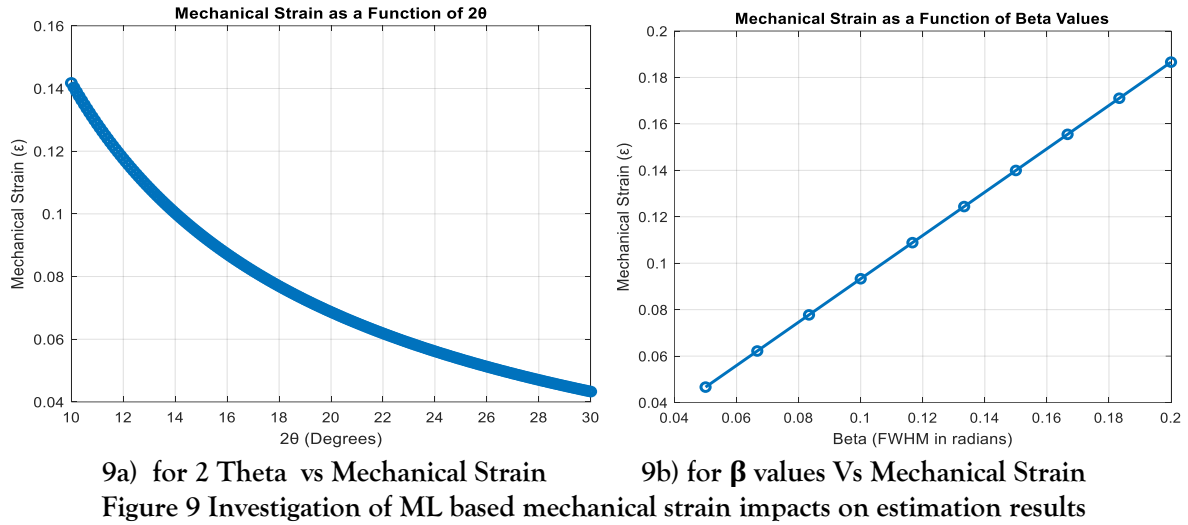


Figure 8: Comparative evaluation of the Beta value vs. crystalline size and strain.

It is found that strain and stress are inversely related to each other. The final predicted crystallite Size from ML Model for regression analysis is Beta = β =0.15 and the respective size is 1.06 nm.



Additionally, the MATLAB simulation in Figure 9 representing the result of investigation of ML based mechanical strain impacts. Figure 9a) shows a negative correlation between mechanical strain (ϵ) and 2θ (degrees). As 2θ increases, mechanical strain decreases. Figure 9b) displays a positive correlation between mechanical strain (ϵ) and β values (FWHM in radians). As β values increase, so does mechanical strain. The mechanical strain is related to the crystalline size as;

$$\epsilon \propto \frac{1}{D} = \frac{K}{D} \quad (7)$$

Where K is a constant, (related to dislocation density), D is the grain size. Thus, as an experiment in this work the β value is varied and respective strain vs crystalline size is predicted using the regression analysis. The Figure 10 presented the comparative predicted results vs actual results for the Linear and proposed polynomial regression model. In this work the third order regression is proposed as per the small set of data. It is clear from the Figure 10 that 3rd order regression or polynomial regression offers close approximation of the actual strain and size data.

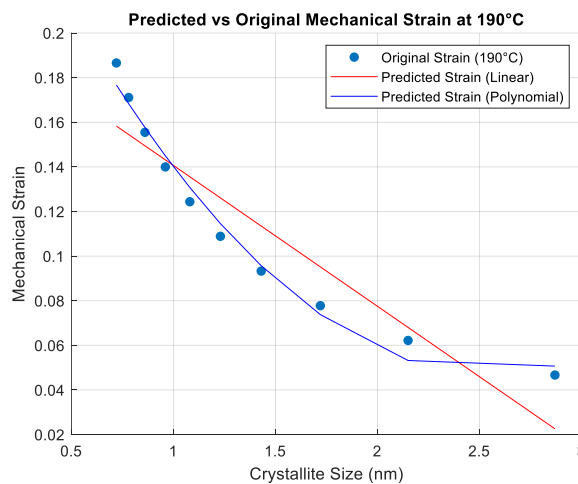


Figure 10 Predicted Strain results vs actual results at 190°C

The Table 6 compares linear regression and polynomial regression in terms of parametric performance using metrics like R-squared, Mean Squared Error, and Sum of Squared Errors. The results show that polynomial regression significantly outperforms linear regression. Polynomial regression achieves a much higher R-squared value (0.9836) compared to linear regression (0.8562), indicating a substantially better fit to the data. Also, it achieves lower MSE and SSE values.

| Method | R square | MSE | SSE |
|-----------------------|----------|------------|--------|
| Linear regression | 0.8562 | 2.8682e-04 | 0.0171 |
| Polynomial regression | 0.9836 | 3.2628e-05 | 0.0196 |

Table 6: Parametric performance of prediction methods

6. CONCLUSIONS AND FUTURE SCOPES

In conclusion, this study successfully synthesized Lanthanum hydroxide and Lanthanum oxide nanoparticles using a simple co-precipitation method at room temperatures. The annealing temperature significantly influenced the morphology and properties of the nanoparticles. This cost-effective approach provides valuable insights into the structural, morphological, and compositional characteristics of nanoparticles, which can be beneficial for various applications in materials science and technology. In This study synthesized nano particles are having grain size 7.13nm and 7.92nm with mechanical strain 0.0294 & 0.051133 respectively. FTIR spectroscopy confirmed the presence of La-O stretching modes, while SEM imaging showed agglomerated nanoparticles with morphological differences between samples synthesized at 160°C and 190°C. EDS analysis provided elemental composition data, with lanthanum and oxygen as the main constituents. The UV-Visible Spectroscopy revealed a significant absorbance peak around 300 nm in the La₂O₃ at 160°C. The annealing temperature was found to significantly impact the morphology, crystallinity, and properties of the resulting nanoparticles.

The ML-based MATLAB simulation was used to predict optimal strain and crystallite size following main conclusions are drawn from the investigation.

- The impact of different β factors on strain and crystallite size was investigated.
- Third-order polynomial regression significantly outperformed linear regression, achieving a higher R-squared value of 0.9836 compared to 0.8562, a lower Mean Squared Error of 3.2628e-05 versus 2.8682e-04, and a slightly better Sum of Squared Errors.
- Strain and stress were found to be inversely related to each other.

Further studies could explore how varying temperature profiles, precursor concentrations, and reaction times affect the properties of the La₂O₃ nanoparticles. This could help optimize the synthesis process for specific applications. Research into scaling up the synthesis process while maintaining nanoparticle quality and reducing production costs could be valuable for industrial applications.

ACKNOWLEDGEMENT

Author here by acknowledges each and every individual who have supported directly or indirectly for the current research and helped the authors.

REFERENCES

- [1]. N.Ramjeyanthi, M.Alagar and Muthuraman, Synthesis, Structural and Optical Characterization of Uncalcined La₂O₃ Nanoparticles by Co-Precipitation Method, International Journal of Interdisciplinary Research and Innovations Vol. 6, Issue 3, pp: (389-395), Month: July - September 2018, Available at: www.researchpublish.com
- [2]. Shinde, K. P., Kim, D.-H., Park, H.-R., Yu, S.-C., Tien, V. M., Huang, L., & Chung, K. C. (2020). Magnetocaloric effect in Tb₂O₃ and Dy₂O₃ nanoparticles at cryogenic temperatures. *Journal of Applied Physics*, 127(5), 054903. <https://doi.org/10.1063/1.5120350>
- [3]. S. Karthikeyan, A. Dhayal Raj, A. Albert Irudayaraj, D. Magimai Antoni Raj, "Effect of "Temperature on the Properties of La₂O₃ Nanostructures, Materials Today: Proceedings, Volume 2, Issue 3, pp. 1021-1025, 2015, <https://doi.org/10.1016/j.matpr.2015.06.030>.
- [4]. P Ram Kumar, T Manimuthu Maharajan, M Chinnasamy, A Pitchiah Prabhu, J Arockia Suthagar and K Santhana Kumar, "Hydroxyl radical scavenging activity of La₂O₃ nanoparticles", The Pharma Innovation Journal 8. pp 59-763.(2019)
- [5]. Subramani Rahul, Amal George, Chinnapparaj Dominic Savio, P.Saravanan, Alphonse DhayalRaj,Savarenathan John Sundaram, Michael Raj Sherlin Nivetha, Sandhanasamy Devanesan, P. Srinivasan and K. Arul,' Time-Dependent Hydrothermal Synthesis of La₂O₃ NPs for Effective Catalytic Activity of Ionic Dye'Luminiscence, Volume39, Issue10, (2024), <https://doi.org/10.1002/bio.4915>
- [6]. Raid A Ismail, Fattin A Fadhil, and Halah H. Rashed,' Novel route to prepare lanthanum oxide nanoparticles for optoelectronic devices' International Journal of Modern Physics B Vol. 34, No. 13, 2050134 (2020). <https://doi.org/10.1142/S0217979220501349>

- [7]. Khandel, P., & Shahi, S. K. (2018). Mycogenic nanoparticles and their bio-prospective applications: current status and future challenges. *Journal of Nanostructure in Chemistry*, 8(4), 369–391. <https://doi.org/10.1007/s40097-018-0285-2>
- [8]. Ahmadi, F., & Lackner, M. (2024). Green Synthesis of Silver Nanoparticles from Cannabis sativa: Properties, Synthesis, Mechanistic Aspects, and Applications. *ChemEngineering*, 8(4), 64. <https://doi.org/10.3390/chemengineering8040064>
- [9]. Joshi, N.C.; Chodhary, A.; Prakash, Y.; Singh, A. Green synthesis and characterization of α -Fe₂O₃ nanoparticles using Leaf Extract of Syzygiumcumini and their suitability for adsorption of Cu(II) and Pb(II) ions. *Asian Journal of Pharmaceutical and Clinical Research* 2019, 31, 809-1814, <https://doi.org/10.14233/ajchem.2019.22024>.
- [10]. Amanullakhan A. Pathan, Kavita R. Desai and C.P. Bhasin, Synthesis of La₂O₃ Nanoparticles Nanoparticles using Glutaric acid and Propylene glycol for Future CMOS Applications, "International Journal of Nanomaterials and Chemistry", 3 (2), (2017), 21-25.
- [11]. Holzwarth, U., Gibson, N. The Scherrer equation versus the 'Debye-Scherrer equation'. *Nature Nanotech* 6, 534 (2011). <https://doi.org/10.1038/nnano.2011.145>
- [12]. G.K. Williamson, W. Hall, "Acta Metallurgica", 1, (1953), 22
- [13]. P. G. Anu Krishna1, Nisha J. Tharayil "Dielectric Properties of Lanthanum Oxide Nanoparticle Synthesized Using Chemical Co-Precipitation Method" AIP Conference Proceedings, 2162, 020079, (2019).
- [14]. Qiuying Mu, Yude Wang, "Synthesis, characterization, shape-preserved transformation, and optical properties of La(OH)₃, La₂O₂CO₃, and La₂O₃ Nanorods", *Journal of Alloys and Compounds* (2011) 509, 396–401.
- [15]. P Ram Kumar, T Manimuthu Maharajan, M Chinnasamy, A Pitchiah Prabu, J Arockia Suthagar and K Santhana Kumar, Hydroxyl radical scavenging activity of La₂O₃ nanoparticles, *The Pharma Innovation Journal* 8 (2019) 59-763.
- [16]. Jayadeep Tejani, Rahul Shah, Hiral Vaghela, Shailesh Vajapara and Amanullakhan Pathan, Controlled Synthesis and Characterization of Lanthanum Nanorods, *Int. J. Thin.Film. Sci. Tec.* 9, 2(2020) 119-125.
- [17]. Pathan, A.A.; Desai, K.R.; Bhasin, C.P. Synthesis of La₂O₃ Nanoparticles Using Glutaric Acid and Propylene Glycol for Future CMOS Applications. *International journal of Nanomaterials and Chemistry* 2017, 3, 21– 25, <http://dx.doi.org/10.18576/ijnc/030201>
- [18]. Khalaf, W.M. & Al-Mashhadani, M.H. (2022). Synthesis and Characterization of Lanthanum Oxide La₂O₃ Net-like Nanoparticles By New Combustion Method. *Biointerface Research in Applied Chemistry*. Volume 12, Issue 3, 2022, 3066 - 3075 <https://doi.org/10.33263/BRIAC123.30663075>
- [19]. Yeosang Yoon, Phuoc Loc Truong, Daeho Lee, Seung Hwan Ko, "Metal-Oxide Nanomaterials Synthesis and Applications in Flexible and Wearable Sensors, *ACS Nanoscience Au*, Vol 2, Issue 2 2021, <https://doi.org/10.1021/acsnanoscienceau.1c00029>
- [20]. Tejani, Jayadip Ghanshyambhai & Shah, Rahul & Vaghela, Hiral & Vajapara, Shailesh & Pathan, Amanullakhan. (2020). Controlled Synthesis and Characterization of Lanthanum Nanorods. *International Journal of Thin Films Science and Technology*. 9. <http://dx.doi.org/10.18576/ijtfst/090205>.
- [21]. Bhautik, P. Review on synthesis of Lanthanum oxide (La₂O₃) and characterization techniques. *Gradiva Review Journal*, Volume 7 Issue 12, pp 260-273, 2021 <https://doi.org/10.1016/J.JALLCOM.2010.09.006>
- [22]. Hanif, Zahra & Jabeen, Nyla & Anwaar, Sadaf & Aftab Malik, Ayesha & Anwar, Tauseef & Qureshi, Huma & Munazir, Mehmooda & Zaman, Wajid & Soufan, Walid. (2024). Synthesis and characterization of Lanthanum Oxide nanoparticles using Citrus aurantium and their effects on Citrus limon Germination and Callogenesis. *Scientific Reports*. 14. <https://dx.doi.org/10.1038/s41598-024-73016-4>
- [23]. Pranali S. Parab, Aniket A. Pawanoji, Komal R. Jarhad, Amol S. Pawar, "Tailoring La₂O₃ Nanomaterials Through Doping and Coating for Improved Photocatalytic Degradation, Catalytic Reduction, and Other Biological Applications", *ChemistrySelect*: Volume 10, Issue 17, e202405740, May 5, 2025, <https://doi.org/10.1002/slct.202405740>
- [24]. K. Parimala Gandhi, S. Hemalatha, S. Sruthi, "Novel Synthesis and Characterization of Lanthanum oxide Nanoparticles from Nano-sized Lanthanum (III) Compound", *J. Environ. Nanotechnol.*, Volume 13, No 2, pp. 01-04, 2024, <https://doi.org/10.13074/jent.2024.06.241538>
- [25]. Tao, H., Wu, T., Aldeghi, M. *et al.* Nanoparticle synthesis assisted by machine learning. *Nat Rev Mater* 6, 701–716 (2021). <https://doi.org/10.1038/s41578-021-00337-5>
- [26]. Velinova R, Kaneva N, Ivanov G, Kovacheva D, Spassova I, Todorova S, Atanasova G, Naydenov A. Synthesis and Characterization of Pd/La₂O₃/ZnO Catalyst for Complete Oxidation of Methane, Propane and Butane. *Inorganics*. 2025; 13(1):17. <https://doi.org/10.3390/inorganics13010017>